

Preparation, Characterization, and Photocatalytic Performance of PANI/ZnO/MWCNT Nanocomposites for Cinnarizine Degradation in Aqueous Solution

MEH Ahamed^{1*}, H. E. Salman¹, A. S. Elsadig², M.H. Awad³

¹Department of Chemistry, College of Science, Sudan University of Science and Technology, Khartoum, Sudan

²Department of science, College of Education, Sudan University of Science and Technology, Khartoum, Sudan

³Department of Chemistry, Faculty of Science and Technology, University of Shendi, Shendi, Sudan

DOI: <https://doi.org/10.36347/sjahss.2026.v14i04.003>

| Received: 23.02.2026 | Accepted: 13.04.2026 | Published: 17.04.2026

*Corresponding author: MEH Ahamed

Department of Chemistry, College of Science, Sudan University of Science and Technology, Khartoum, Sudan

Abstract

Original Research Article

In this study, polyaniline/zinc oxide/multi-walled carbon nanotube (PANI/ZnO/MWCNT) nanocomposites containing varying amounts of MWCNTs (0.1, 0.3, and 0.5 g) were successfully synthesized via in situ oxidative polymerization combined with a co-precipitation method. The prepared nanocomposites were characterized using Fourier transform infrared spectroscopy (FTIR), UV-visible spectroscopy, and scanning electron microscopy (SEM). FTIR analysis confirmed the presence of characteristic functional groups corresponding to PANI, ZnO, and MWCNTs, indicating successful composite formation. SEM images revealed homogeneous coating of ZnO and MWCNTs by the PANI matrix. Optical studies showed that incorporation of MWCNTs slightly reduced the band gap energy, enhancing light absorption. The photocatalytic performance of the nanocomposites was evaluated for the degradation of cinnarizine in aqueous solution under sunlight irradiation. The degradation efficiency increased with increasing MWCNT content, reaching a maximum of 86.1% using the composite containing 0.5 g MWCNTs at an initial cinnarizine concentration of 17 µg/mL after 40 minutes of irradiation. Kinetic analysis indicated pseudo-first-order behavior. These results demonstrate that PANI/ZnO/MWCNT nanocomposites are promising photocatalysts for the treatment of pharmaceutical wastewater.

Keywords: Photocatalysis; Cinnarizine; MWCNTs; Polyaniline; Nanocomposites.

Copyright © 2026 The Author(s): This is an open-access article distributed under the terms of the Creative Commons Attribution 4.0 International License (CC BY-NC 4.0) which permits unrestricted use, distribution, and reproduction in any medium for non-commercial use provided the original author and source are credited.

1. INTRODUCTION

Pharmaceutical residues are now frequently found in aquatic systems, largely because conventional wastewater treatment processes do not completely eliminate them. Their persistence in water bodies can negatively affect aquatic life and may also pose risks to human health. In recent years, significant research has focused on the breakdown of harmful organic pollutants in wastewater using semiconductor-based photocatalysis (Chen *et al.*, 2002). Certain pharmaceutical contaminants, including cinnarizine, can be degraded through photocatalytic processes into less toxic substances. This highlights the promise of semiconductor materials combined with ultraviolet light as an effective approach for wastewater treatment. The efficiency of degradation processes is influenced by chemical composition, biological factors, and environmental conditions such as climate. Photocatalytic

reactions are generally categorized as either homogeneous or heterogeneous, depending on the nature of the reactants and catalysts involved. Owing to its effectiveness and environmental relevance, semiconductor photocatalysis has gained considerable attention as a method for addressing pollution challenges (Fujishima, Rao and Tryk, 2000).

ZnO is semiconductor nanoparticles as one of the most important photocatalysts, because it is widely used in the degradation and complete mineralization of environmental pollutants (Dutta and Basak, 2009). The combination of inorganic semiconductor with conjugated polymer to increase photo reactivity is an emerging area of research (Pei *et al.*, 2014; Gilja *et al.*, 2017, 2018). Polyaniline (PANI) is one of the most important conducting polymers because of its properties such as easy synthesis, environmental and chemical

stability, low cost, relatively high conductivity and unique redox behavior (Wang *et al.*, 2010; Qin *et al.*, 2018).

Cinnarizine is a pharmaceutical agent with multiple therapeutic uses, including its role as an antihistamine and a calcium channel blocker, as well as its application in managing both cerebral and peripheral vascular insufficiency. It is also commonly prescribed to prevent motion sickness and to treat vestibular disorders arising from various causes. The drug has demonstrated effectiveness in conditions such as Meniere's disease, an inner ear disorder, and vertigo associated with cerebrovascular issues (Kirtane *et al.*, 2019).

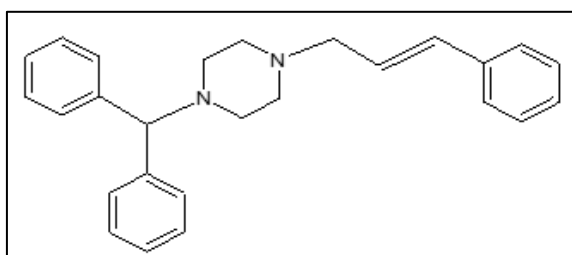


Figure 1: structure of cinnarizine

Side effects experienced while taking cinnarizine range from mild to quite severe. Possible cases of hypersensitivity reactions, as well as movement problems, muscle rigidity, tremor, and also cases of drowsiness, sweating, dry cases of headache and dry mouth, skin problems, lethargy, gastrointestinal irritation (Hassan *et al.*, 2002). In this work, PANI/ZnO/MWCNTs nanocomposites were synthesized and evaluated for photocatalytic degradation of cinnarizine in aqueous solution under sunlight irradiation at different concentrations (Wang, Tade and Shao, 2015).

2. Experimental

2.1 Materials

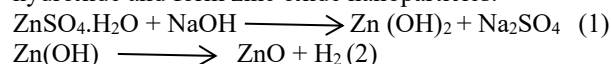
Cinnarizine was kindly provided by the Shanghai-Sudan pharmaceutical company. All chemicals used were analytical grade and were used without any further purification. Sodium hydroxide NaOH (Gynggido, Korea), zinc sulfate monohydrate ZnSO₄.H₂O (Mumbai, India), zinc acetate dihydrate Zn(CH₃COO)₂.2H₂O (India), aniline AR (99.5%) (New Delhi, India), hydrochloric acid HCl (36-38%) (Gynggido, Korea), ammonium persulfate (APS) (NH₄)₂S₂O₈ (98%) (Mumbai, India), and methanol AR (Mumbai, India).

2.2 Synthesis of Nanocomposites

2.2.1 Preparation of ZnO Nanoparticles

ZnO nanoparticles were prepared using an aqueous solution method (Saravanan *et al.*, 2013). One hundred twenty-five cm³ of 1M zinc sulfate monohydrate solution was placed in a 500 cm³ beaker under continuous stirring. After 30 minutes of stirring, 125 cm³ of 1M sodium hydroxide was added dropwise,

and the addition was completed at 10 min. Then, 150 cm³ of distilled water was added to the solution. The solution was stirred vigorously at 600 rpm for 5 hrs.; zinc hydroxide (milky solution) was formed and kept at 80 °C for 5 hrs. in an oven. The white precipitate was filtered and washed with ethanol and distilled water several times and then dried at room temperature. The collected powder was calcined at 200°C for 2 hrs. to remove hydroxide and form zinc oxide nanoparticles.



2.2.2 Preparation of Polyaniline (PANI)

Polyaniline (PANI) was prepared following (Gilja, Vrbanc *et al.*, 2018). 0.3 M of pure aniline was dissolved in 100 cm³ of 1M HCl aqueous solution. After cooling the solution to 5°C, 0.35 M of APS solution dissolved in 1M HCl was added dropwise to the aniline solution for about 15 minutes. The color of the solution changed from clear to green, indicating PANI formation. The solution was stirred continuously at 5°C for 3 hrs. to complete polymerization. The green precipitate was filtered and washed with distilled water and methanol several times to remove any impurities and residual unreacted monomers, then dried at room temperature for 96 hrs.

2.2.3 Preparation of PANI/ZnO composite

PANI/ZnO nanocomposite was prepared according to (Das and Sarkar 2017) with slight modification. 0.3 M of aniline was dissolved in 100 cm³ of 1M HCl solution. 0.35 M of APS solution was added dropwise to the aniline solution for about 15 minutes. The color of the solution changed from clear to green, indicating PANI formation. The solution was then stirred for 2 hrs. In the same solution, 0.3M zinc acetate dihydrate and 0.3M NaOH were added slowly and stirred for two more hours to form a ZnO-PANI nanocomposite. The dark green precipitate was filtered and washed with distilled water and methanol several times to remove any impurities and residual unreacted monomers, then dried at room temperature for 48 hrs.

2.2.4 Preparation of PANI/ZnO /MWCNTs composite

PANI/ZnO /MWCNTs composite was prepared by in-situ polymerization. 0.3 M of aniline was dissolved in 100 cm³ of HCl aqueous solution. A desired amount of multiwalled carbon nanotubes (MWCNTs) (0.1, 0.3, or 0.5 g) was added to aniline solution under ultrasonic for 10 minutes. 0.35 M of APS solution was added dropwise to the mixture containing aniline and MWCNTs, and the addition was completed for about 15 minutes. The solution was then stirred for 3 hrs. In the same solution, 0.3M zinc acetate dihydrate and 0.3M NaOH were added slowly and stirred for two more hours to form ZnO/PANI/MWCNTs nanocomposite. The precipitate was filtered and washed with distilled water and methanol several times to remove any impurities and

residual unreacted monomers, then dried at room temperature for 96 hrs (Li *et al.*, 2016).

2.3 Characterization methods

Fourier transform infrared spectroscopy (FT-IR) spectra were recorded on a Shimadzu, Japan, using potassium bromide pellets in the range of 400–4000 cm^{-1} . A multipoint baseline correction was made for all the FTIR spectra. The morphology of as-prepared composites was examined with a scanning electron microscope (SEM, Vega3 Tescan, Czech) after coating with a thin layer of gold under reduced pressure. The UV-visible spectra of as-prepared composites were recorded using a UV-Vis double-beam spectrophotometer (model LT-2700, India). The absorption spectra of dilute solutions of composites in distilled water ($\sim 200 \text{ mg/dm}^3$) were scanned at a wavelength from 200 to 400 nm. A UV-Vis single-beam spectrophotometer (model 1240, Shimadzu, Japan) was utilized to measure the concentration of cinnarizine. A sensitive balance (Shimadzu, Japan), a hotplate with stirrer (Scott Science, model LMS-1003, UK), an ultrasonic cleaner (UC-02, China), and a pH meter (model 3505, Jenway, UK) were used in composites and solutions preparation. A drying oven (Acer No. 954, India) was used to dry the composites.

2.4 Photocatalytic degradation of cinnarizine

2.4.1 Preparation of stock solution of cinnarizine

The stock solution of cinnarizine was prepared in 0.1M HCl. Accurately weighed 8.5 mg of cinnarizine was dissolved in a 100 cm^3 volumetric flask and sonicated for about 5 minutes. Then dilution was made by taking 10 cm^3 of stock solution and dissolving it in 50 cm^3 of 0.1M HCl to obtain a concentration of 17 $\mu\text{g/cm}^3$. The solution of the sample was scanned over the wavelength range from 200 to 400 nm. The λ_{max} of cinnarizine was found to be 253 nm.

2.4.2 Linearity

From the stock solution, different concentrations from 6.8 to 27.2 $\mu\text{g/cm}^3$ of sample were prepared. Absorbance of all the dilutions was determined at λ_{max} 253 nm. Then the absorbances were plotted against the respective concentrations to obtain the standard calibration curve.

2.4.3 Photocatalytic degradation studies

The photocatalytic degradation experiments were carried out using 50 cm^3 beakers under a sunlight source. 17.5 mg of the catalyst (catalyst dosage of 0.7 g/dm^3) was added to 25 cm^3 of cinnarizine sample solution with different initial concentrations of 25.5, 18.7, 15.3 and 11.9 $\mu\text{g/cm}^3$. The solution was magnetically stirred in the dark for 1 hr. to reach the adsorption-desorption equilibrium. Then it was exposed to sunlight with a total duration of 40 min. 3 cm^3 aliquots of the solutions were withdrawn at different times and centrifuged for 20 minutes at 10,000 rpm. After

separation, the aliquots of the solutions were analyzed using a UV-Vis spectrophotometer at 253 nm.

3. RESULTS AND DISCUSSION

3.1 Preparation of PANI/ZnO/MWCNT by in-situ polymerization

The aniline polymerized in the presence of MWCNTs, resulting in a PANI-coated MWCNT structure. The formation of a PANI-coated MWCNT morphology for MWCNT/PANI composites when aniline is polymerized in the presence of MWCNT has been studied by Saini *et al.*, (Saini, Choudhary *et al.*, 2009). When the nanocomposite is being prepared, a weak charge transfer complex is created because aniline is an electron donor and MWCNT is an electron acceptor (Tseng, Baker *et al.*, 2007). The aniline monomer's lone pair of electrons aids in the complex's creation. With a portion of the aniline in the solution phase and others on the MWCNTs' surface, a heterogeneous system develops. Polymerization occurs on the surface of MWCNTs as well as in solution (bulk polymerization) with the addition of the oxidant. Further, the catalytic activity of the MWCNTs promotes the formation of cation radicals on the surface of MWCNTs, which leads to a greater rate of polymerization on the MWCNT surface, leading to polymer-coated MWCNT morphology of the composite.

The aniline polymerized in the presence of MWCNTs, resulting in a PANI-coated MWCNT structure. The formation of a PANI-coated MWCNT morphology for MWCNT/PANI composites when aniline is polymerized in the presence of MWCNT has been studied by Saini *et al.*, (Saini, Choudhary *et al.*, 2009). When the nanocomposite is being prepared, a weak charge transfer complex is created because aniline is an electron donor and MWCNT is an electron acceptor (Tseng, Baker *et al.*, 2007). The aniline monomer's lone pair of electrons aids in the complex's creation. With a portion of the aniline in the solution phase and others on the MWCNTs' surface, a heterogeneous system develops. Polymerization occurs on the surface of MWCNTs as well as in solution (bulk polymerization) with the addition of the oxidant. Further, the catalytic activity of the MWCNTs promotes the formation of cation radicals on the surface of MWCNTs, which leads to a greater rate of polymerization on the MWCNT surface, leading to polymer-coated MWCNT morphology of the composite.

On the other hand, ZnO NPs and MWCNTs both function as electron acceptors, and PANI as an electron donor, during the in-situ polymerization process used to produce the three-component nanocomposite. This is due to the slight positive charge created on PANI and a slight negative charge developed on ZnO (Tseng, Baker *et al.*, 2007, Feng, Li *et al.*, 2011). The schematic for preparation PANI/MWCNTs/ZnO is depicted in Figure 2.



Figure 2: Preparation of PANI/ZnO/MWCNT by in-situ polymerization

3.2 Fourier Transform – infrared spectroscopy (FT-IR) Analysis

FT-IR data is a feature of a particular compound that provides information about its functional groups. All

catalysts were successfully prepared and the results were as shown in Table 1.

Table 1: shows FT-IR spectrum of the catalyst

Material	O-H	N-H	C-H	C=C	C-C	C-N	C-O	Zn-O
Zinc oxide	3412 st.vib & 1569 bending	-	-	-	-	-	-	435, 648, & 616
Polyaniline	-	3437 st.vib & 1574 bending	924 bending	-	1410	1340 & 1140	1018	-
PANI/ZnO nanocomposite	-	3427 st.vib & 1572 bending	924	-	1413	1340 & 1150	-	648
MWCNTs	3421	-	921	1569 bend	1343	-	1018 bend	-
PANI/ZnO /MWCNTs (0.1g)	-	3417	918	1569	1410	1340 & 1137	1014	648
PANI/ZnO /MWCNTs (0.3g)	-	3434	924	1569	1413	1340 & 1127	1021	619 & 657
PANI/ZnO /MWCNTs (0.5g)	-	3427	924	1569	1410	1343	1014	648

Table 1 and Figure 3 show that the FTIR spectra data confirmed the presence of characteristic peaks of PANI (N-H, C-N), ZnO (Zn-O), and MWCNTs (C=C, O-H). Slight peak shifts indicated interactions between the composite components.

In the FT-IR of ZnO the main characteristic peaks of ZnO nanoparticles appeared at 3412 and 1569 cm^{-1} are attributed to O-H stretching and bending vibration, respectively, while the peaks at 648 and 616 cm^{-1} are related to Zn-O-Zn, but the peak at 435 cm^{-1} is due to Zn-O stretching bond.

In FT-IR of pristine PANI, the characteristic peaks at 3437 cm^{-1} and 1574 cm^{-1} were assigned to N-H stretching and bending vibrations respectively, while the peaks appeared at 1340 cm^{-1} and 1140 cm^{-1} were

attributed to C-N stretching vibration, but at 924 cm^{-1} was due to C-H bend out of plane.

In the PANI/ZnO nanocomposite FT-IR spectra, the corresponding peaks of pure PANI at 3437 and 1574 cm^{-1} were shifted to lower wavenumber to 3427 and 1572 cm^{-1} respectively. This shift is due to interaction between Polyaniline chain and ZnO nanoparticles. While the peaks at 1140 cm^{-1} was shifted to longer wave number to 1150 cm^{-1} . The new peak appeared at 648 cm^{-1} is due to appearance of Zn-O in nanocomposite.

The main characteristic peaks of oxidized multi walled carbon nanotube MWCNTs appeared at 3421 and 1018 cm^{-1} can be assigned to O-H and C-O stretching vibrations of carboxylic acid, while peak at 1569 and 1343 cm^{-1} due to C=C and C-C stretching vibration.

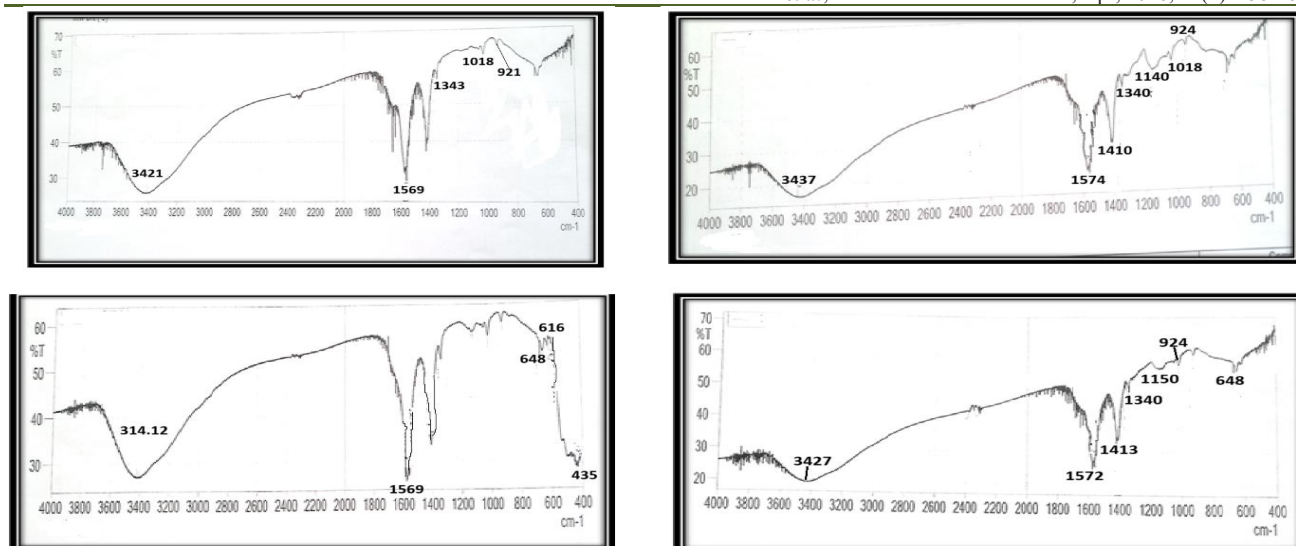


Figure 3: FT-IR of MWCNTs (a), PANI (b), ZnO (c), and ZnO/MWCNTs.

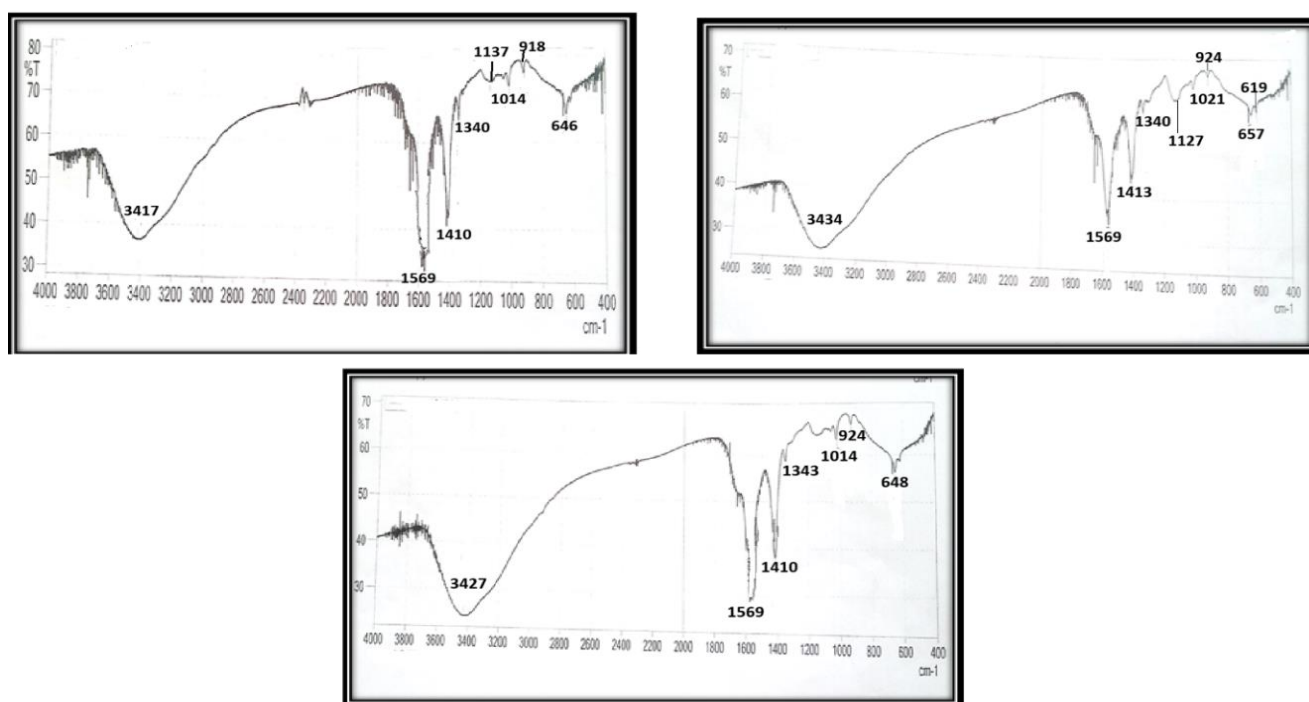


Figure 4: FT-IR of PANI/ZnO/ MWCNTs (0.1 g) (a), PANI/ZnO/ MWCNTs (0.3 g) (b), and PANI/ZnO/ MWCNTs (0.5 g) (c),

The FT-IR spectra of PANI/ZnO/MWCNTs composites containing 0.1, 0.3, and 0.5 g of MWCNTs show the main characteristic peaks compared to the corresponding peaks of PANI/ZnO nanocomposite. In of composite with 0.1 g of MWCNTs, the peaks appeared at 3417, 1340, 1340, 1137, 918, and 648 cm^{-1} are due to N-H, C-N st. vib., C-H bend, and Zn-O st. vib., respectively. However, in the composite containing 0.3 g of MWCNTs, some peaks were shifted to higher wavenumbers at 3434, 1021, 1413, and 657 cm^{-1} , while other peaks shifted to lower wavenumbers at 1127 cm^{-1} .

For the composite containing 0.5 g of MWCNTs, slight shifts appeared at 1343 cm^{-1} (C-N), while the peaks 3427, 1014, 1569, and 648 cm^{-1} showed no change in wavenumber. The successful formation of PANI/ZnO/MWCNTs are approved by the appearance of N-H, C-H, and C-N bonds of PANI, Zn-O, and C=C bonds of oxidized MWCNTs.

3.3 Optical properties

UV-Vis. absorption spectra were used to determine the optical properties of the catalysts were shown in Table 2

Table 2: shows optical properties of catalysts

Catalyst	λ_{\max} (nm)	Abs. coefficient(cm^{-1})	Band gap(eV)
ZnO	305	4.6×10^2	3.60
PANI	265	4.58×10^2	3.99
MWCNTs	240	4.54×10^2	4.28
PANI/ZnO	220 285	4.6×10^2 3.91×10^2	3.98
PANI/ZnO/MWCNTs 0.1g	220 285	5.18×10^2 4.41×10^2	3.98
PANI/ZnO/MWCNTs 0.3 g	220 285	5.76×10^2 4.95×10^2	3.94
PANI/ZnO/MWCNTs 0.5 g	220 285	6.53×10^2 5.56×10^2	3.92

UV-Vis. analysis showed absorption in the UV region. Incorporation of MWCNTs slightly reduced the band gap energy from 3.98 eV to 3.92 eV, indicating

improved charge transfer and enhanced photocatalytic performance.

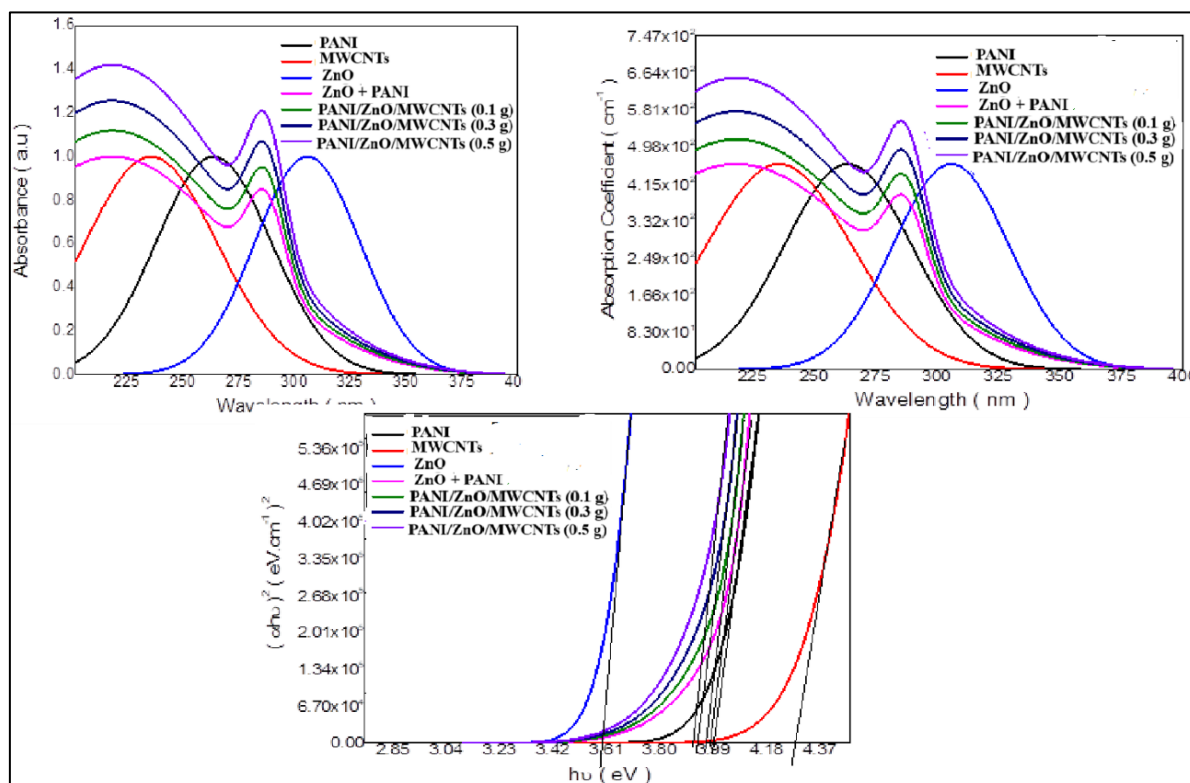


Figure 5: The relationship between absorbance (a.u) and wavelength (a), the absorption coefficient (cm^{-1}) versus wavelength (b) and the band gap energy (eV) (c) of PANAI, MWCNTs, ZnO, ZnO + PANI, PANI/ZnO/MWCNTs (containing 0.1g, 0.3 g and 0.5 g of MWCNTs).

All the catalysts were absorbed at the UV-region and few light transmit in the visible region, the λ_{\max} absorption of ZnO nanoparticle at 305nm, PANI at 265nm, MWCNTs at 240nm, while in PANI/ZnO nanocomposite the λ_{\max} was appeared at two wavelength 220 and 285 nm, but PANI/ZnO/MWCNTs nanocomposite the λ_{\max} was appeared at the same wavelength 220 and 285 nm but at changed in absorbance.

The absorbance coefficient (α) of all catalysis can be calculated from this simple equation:

$$\text{Absorbance coefficient } (\alpha) = 2.303A/t \quad (3)$$

Where (A) is absorbance and (t) is thickness of thin film. All results were found to be at $(102) \text{ cm}^{-1}$, which means

an indirect transition from the conduction band to the excitation band. Therefore, the electron needs exposure to light to transition.

The optical band gap energy of the catalysts can be evaluated from their fundamental absorption behavior using the Tauc relation, which is expressed as: $\alpha h\nu = B(h\nu - E_g)^n \quad (4)$

Where α is the absorption coefficient, $h\nu$ is the photon energy, E_g is the band gap energy, B is the material constant and $n=2$ due to an indirect allowed transition. Therefore, plotting the straight line of $(\alpha h\nu)^2$ versus $(h\nu)$, or by direct calculation from the following equation: $E_g \text{ (eV)} = 1240/\lambda \quad (5)$

Where, λ is wavelength (nm) corresponding to the absorption edge (Tauc, 1968; Pankove, 1971).

The band gap energy is the region forbidden for the electron. The gap between the valence and the conduction bands increases with the decreasing particle size, and this explains the effect of increasing the amount of MWCNTs from 0.1, 0.3, and 0.5g in the prepared PANI/ZnO/MWCNTs nanocomposite on decreasing the band gap from 3.975, 3.941, and 3.921 eV respectively.

3.4 Morphology of PANI/ZnO/MWCNT

Figure 6 (a-d) displays the SEM images of MWCNTs and PANI/ZnO/MWCNTs containing 0.1, 0.3, and 0.5 g of MWCNTs. A homogeneous coating of MWCNTs/ZnO with PANI with some white rods was seen. The observed white dots on composite surfaces originated from formed MWCNTs and ZnO particles. We also noticed that the rods become more compact on the composite surfaces as MWCNTs content increases due to the aggregation of MWCNTs on the composite's material (Figure 6d).

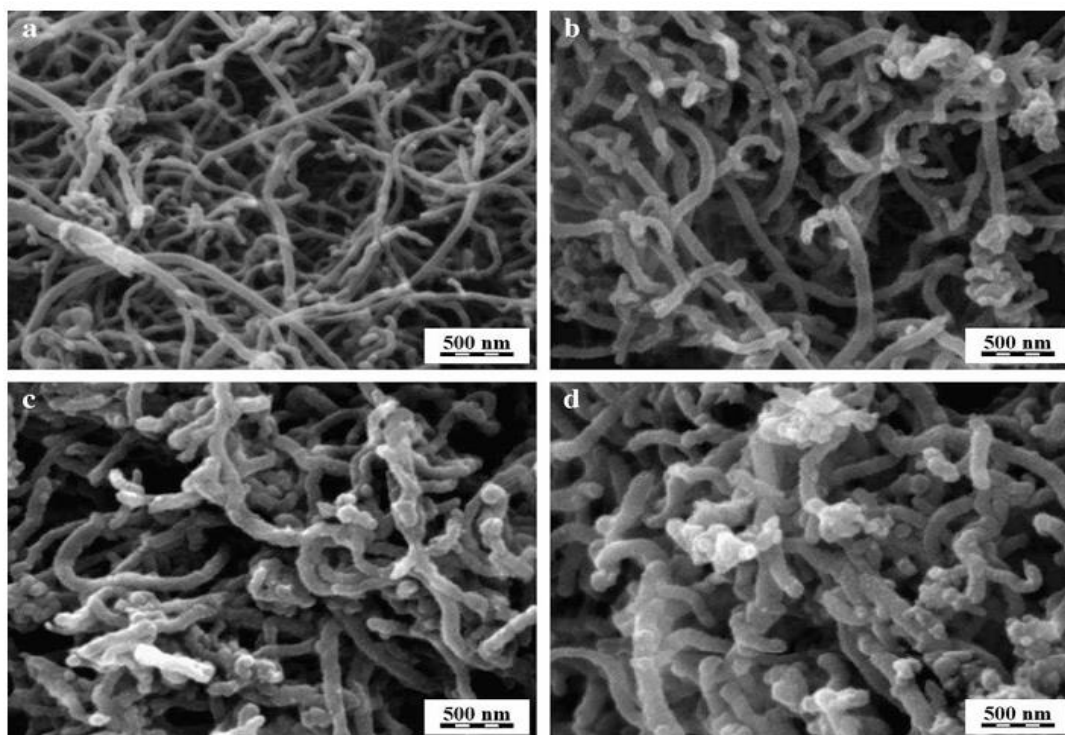


Figure 6 Pristine MWCNT (a), PANI/ZnO/ MWCNT (0.1g) (b), PANI/ZnO/ MWCNT (0.3g), (c) and PANI/ZnO/ MWCNT (0.5g) (d).

SEM images revealed homogeneous distribution of ZnO nanoparticles within the PANI matrix and good dispersion of MWCNTs. Increasing MWCNT content led to a more compact structure.

3.5 Photocatalytic degradation studies

3.5.1 Effect of Irradiation time

Figure 7 shows the photodegradation efficiency of cinnarizine by PANI/ZnO/MWCNTs nanocomposite as catalyst under sunlight. The efficiency is calculated by the following equation:

$$\text{Photodegradation efficiency \%} = (C_0 - C_t) / C_0 \times 100 \quad (4)$$

Where C_0 and C_t are the initial concentration and after irradiation at selected time interval of the Cinnarizine, respectively.

As can be observed, the sample is rapidly degraded by the catalyst in the first 20 minutes of exposure. After 40 min, the observed maximum degradation efficiency of Cinnarizine is about 79.37, 86.1, and 84.4% at 0.5g of PANI/ZnO/MWCNTs nanocomposite and concentration of sample 13.6, 17 and 20.4 $\mu\text{g}/\text{cm}^3$, respectively. That means, the degradation of the sample increases with an increase in the weight of MWCNTs in the nanocomposite, resulting in the improvement of photocatalytic activity. This can be attributed to an increase in specific surface area leading to higher interaction between the (PANI/ZnO/MWCNTs nanocomposite) photocatalyst and sample solution. The best degradation of the sample is appearance at a concentration of 17 $\mu\text{g}/\text{cm}^3$ (86.1%).

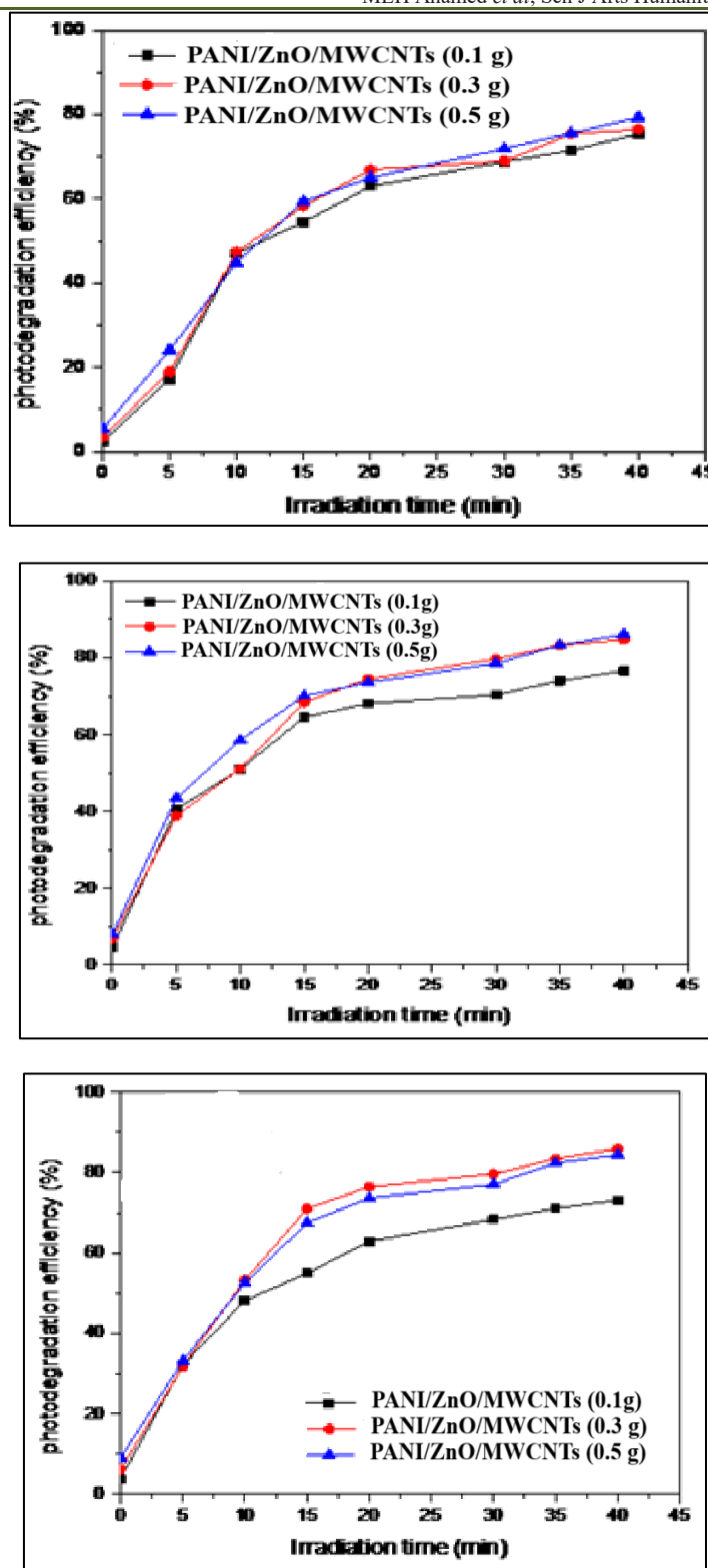


Figure 7 Effect of irradiation time on the photodegradation efficiency of cinnarizine by 0.1, 0.3 and 0.5 g of PANI/ZnO/MWCNTs nanocomposite under sunlight, $C_{catalyst}=0.7g/dm^3$, and sample concentration of a) 13.6, b) 17, and c) 20.4 $\mu g/cm^3$

The plot of $(\ln C_0/C_t)$ versus irradiation time shown in Figure 8 gave first order rate constants of $R_2 > 0.9$. The half-time ($t_{1/2}$) of photodegradation efficiency was calculated using the equation:

$$t_{1/2} = \ln 2 / K_{app} = 0.6931 / K_{app} \quad (8)$$

It was observed that the halves times of photodegradation of Cinnarizine became shorter as the

amount of MWCNTs in the composite increased from 0.1 to 0.5 g. This could be due to an improvement of the

surface area of the nanocomposite with an increase of the weight of MWCNTs.

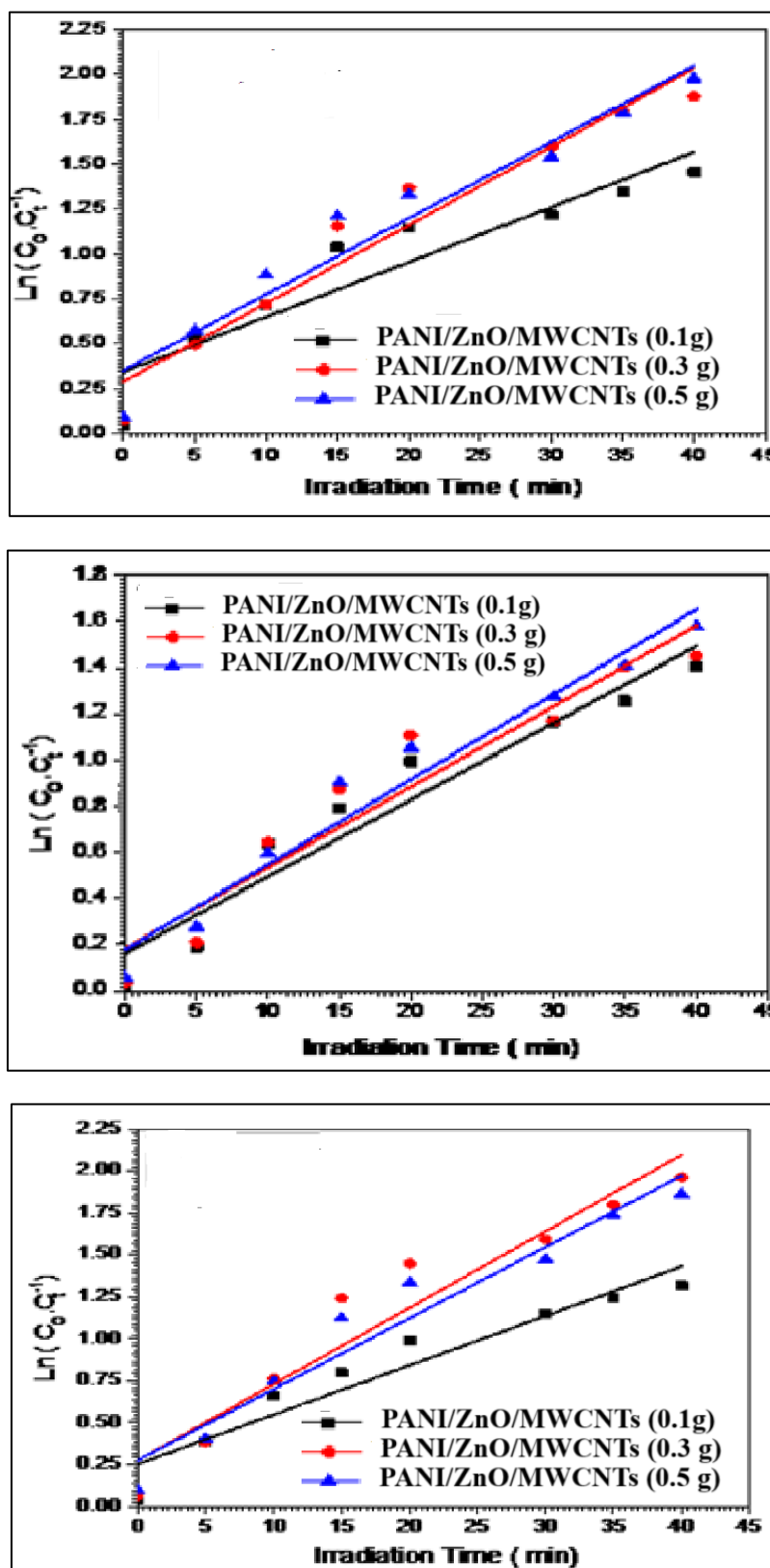


Figure 8: photocatalytic degradation of cinnarizine by 0.1, 0.3 and 0.5 g of PANI/ZnO/MWCNTs nanocomposite under sunlight, and sample concentration of a) 13.6, b) 17, and c) 20.4 $\mu\text{g}/\text{cm}^3$

Table 3: shows apparent rate constants (K_{app}), linear regression coefficients, and half time of Cinnarizine.

No	Photocatalyst	Degradation efficiency %	R^2	$K_{app}(\text{min}^{-1})$	$t_{1/2}(\text{min})$
At concentration 13.6 $\mu\text{g}/\text{cm}^3$					
1	PANI/ZnO/MWCNTs (0.1g)	75.4	0.923	0.03328	20.83
2	PANI/ZnO/ MWCNTs (0.3g)	76.54	0.907	0.03494	19.84
3	PANI/ZnO/ MWCNTs (0.5g)	79.37	0.954	0.03683	18.82
At concentration 17 $\mu\text{g}/\text{cm}^3$					
1	PANI/ZnO/MWCNTs (0.1g)	76.6	0.8513	0.03061	22.64
2	PANI/ZnO/ MWCNTs (0.3g)	84.69	0.937	0.04363	15.89
3	PANI/ZnO/ MWCNTs (0.5g)	86.1	0.9223	0.0424	16.35
At concentration 20.4 $\mu\text{g}/\text{cm}^3$					
1	PANI/ZnO/ MWCNTs (0.1g)	73.2	0.9106	0.02943	23.55
2	PANI/ZnO/ MWCNTs (0.3g)	85.9	0.9173	0.04555	15.22
3	PANI/ZnO/MWCNTs (0.5g)	84.4	0.9375	0.04237	16.36

3.5.2 Effect of initial concentration of sample

The initial concentration of the sample is one of the important factors which needs to be taken into account because it affects the degradation efficiency.

Table 4: Effect of initial concentration of cinnarizine on the degradation efficiency ($C_{\text{sample}} = 25.5, 18.7, 15.3$ and $11.9 \mu\text{g}/\text{cm}^3$, for 40 minutes).

Concentration ($\mu\text{g}/\text{ml}$)	PANI/ZnO/MWCNTs (0.1g)	PANI/ZnO/MWCNTs (0.3g)	PANI/ZnO/MWCNTs (0.5g)
25.5	75.86	78.53	80.98
18.7	77.38	79.94	82.19
15.3	77.81	80.87	82.78
11.9	79.26	81.27	83.28

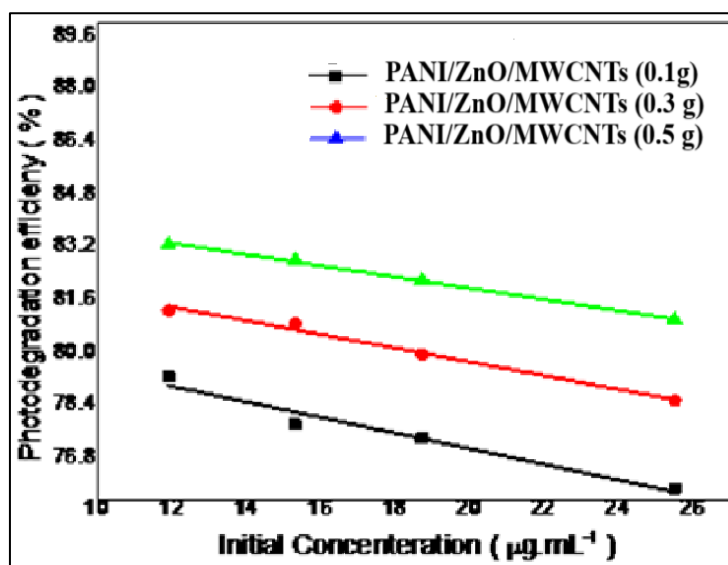
**Figure 9: Effect of initial concentration on photodegradation efficiency of cinnarizine by 0.1, 0.3 and 0.5 g of PANI/ZnO/ MWCNTs nanocomposite under sunlight irradiation at constant ($C_{\text{catalyst}}=0.7\text{g}/\text{l}$, and time =40min).**

Figure 9 shows that the photodegradation efficiency depends on the initial concentration of the sample. When at the initial concentration of a sample, more organic substances are adsorbed on the surface of the catalyst, whereas a smaller number of photons are available to reach the catalyst surface and therefore less $\text{OH}\cdot$ are formed, thus resulting in lower photodegradation percentages.

3.5.3 Effect of doping with MWCNTs

The photocatalytic activity of doping PANI/ZnO nanocomposite with different amounts of MWCNTs (0.1, 0.3, and 0.5 g) increases with decreasing the band gap energy to 3.975, 3.941, and 3.921 eV respectively. Hence, the photodegradation efficiency of cinnarizine doped with 0.1, 0.3, and 0.5 g of MWCNTs was increased in the order of 76.6, 84.69, and 86.1%

respectively, at optimum concentration ($17 \mu\text{g}/\text{cm}^3$) and exposure time of 40 min.

3.6 3.3. Suggestion mechanism of Cinnarizine degradation by the PANI/ZnO/MWCNTs composite

Upon sunlight irradiation, ZnO generates electron-hole pairs. The photogenerated holes react with water to produce hydroxyl radicals ($\bullet\text{OH}$), while

electrons react with oxygen to form superoxide radicals ($\text{O}_2\bullet^-$). These reactive species attack cinnarizine molecules, leading to their degradation into smaller, less harmful intermediates. PANI and MWCNTs enhance charge separation and reduce electron-hole recombination, thus improving photocatalytic efficiency.

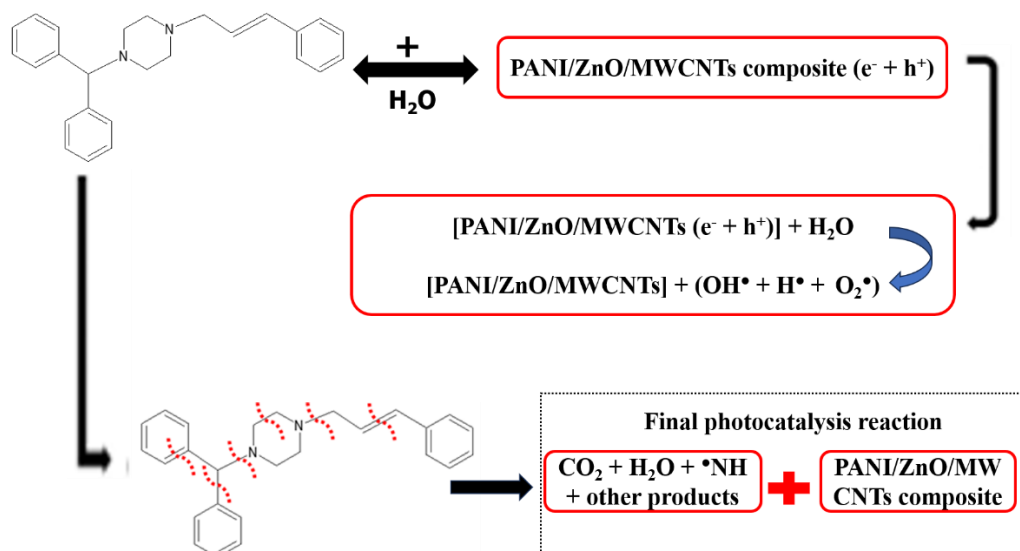


Figure 10: Mechanism of Cinnarizine degradation by the PANI/ZnO/MWCNTs composite

4. CONCLUSION

PANI/ZnO/MWCNTs nanocomposites were successfully synthesized and characterized. The incorporation of MWCNTs improved optical properties and photocatalytic performance. The composite containing 0.5 g MWCNTs demonstrated the highest degradation efficiency (86.1%) for cinnarizine under sunlight irradiation. The study confirms that PANI/ZnO/MWCNTs nanocomposites are promising materials for pharmaceutical wastewater treatment.

REFERENCES

- Chen, X. and Mao, S.S., 2002. Titanium dioxide nanomaterials: Synthesis, properties, modifications, and applications. *Chemical Reviews*, 107(7), pp.2891–2959.
- Das, S. and Sarkar, D., 2017. Synthesis and characterization of polyaniline/ZnO nanocomposites for enhanced photocatalytic applications. *Journal of Environmental Chemical Engineering*, 5(5), pp.4828–4837.
- Dutta, P.K. and Basak, S., 2009. Zinc oxide nanoparticles as an effective photocatalyst for degradation of environmental pollutants. *Journal of Environmental Chemical Engineering*, 1(1–2), pp.23–29.
- Feng, W., Li, L., Yang, Y., Wang, Y. and Zhang, H., 2011. Synthesis and characterization of ZnO/polyaniline nanocomposites with enhanced photocatalytic activity. *Materials Letters*, 65(4), pp.617–620.
- Fujishima, A., Rao, T.N. and Tryk, D.A., 2000. Titanium dioxide photocatalysis. *Journal of Photochemistry and Photobiology C: Photochemistry Reviews*, 1(1), pp.1–21.
- Gilja, V., Novaković, K., *et al.*, 2017. Synthesis and characterization of polyaniline/ZnO nanocomposites for photocatalytic applications. *Applied Surface Science*, 424, pp.245–252.
- Gilja, V., Novaković, K., *et al.*, 2018. Enhanced photocatalytic performance of ZnO–polyaniline composites under visible light. *Materials Chemistry and Physics*, 212, pp.323–330.
- Gilja, V., Vrban, I., Novaković, K., Hrnjak-Murgić, Z. and Kovačević, G., 2018. Synthesis and characterization of polyaniline and its nanocomposites for photocatalytic applications. *Materials Chemistry and Physics*, 212, pp.323–330.
- Hassan, M.A., Ahmed, I.S. and El-Sayed, M.A., 2002. Adverse effects and tolerability of cinnarizine in clinical use. *International Journal of Clinical Pharmacology and Therapeutics*, 40(5), pp.210–216.
- Kirtane, M.V., Bhandari, A., Narang, P. and Santani, R., 2019. Cinnarizine: A contemporary review. *Indian Journal of Otolaryngology and Head & Neck Surgery*, 71(Suppl 2), pp.1060–1068.
- Li, X., Wang, H., Zhang, Y., Liu, Y. and Zhao, H., 2016. Synthesis and enhanced photocatalytic

- activity of polyaniline/ZnO/multiwalled carbon nanotube nanocomposites. *Applied Surface Science*, 369, pp.396–404.
- Pei, S., Cheng, H.M., *et al.*, 2014. The combination of inorganic semiconductors with conjugated polymers for enhanced photocatalytic activity. *Journal of Materials Chemistry A*, 2(37), pp.15561–15569.
 - Qin, Y., Wang, X. and Li, Z., 2018. Advances in polyaniline-based materials for environmental applications. *Journal of Cleaner Production*, 172, pp.443–456.
 - Saini, P., Choudhary, V., Singh, B.P., Mathur, R.B. and Dhawan, S.K., 2009. Polyaniline–multiwalled carbon nanotube nanocomposites for electromagnetic interference shielding and enhanced electrical conductivity. *Synthetic Metals*, 159(23–24), pp.2513–2519.
 - Saravanan, R., Karthikeyan, S., Gupta, V.K., Sekaran, G., Narayanan, V. and Stephen, A., 2013. Enhanced photocatalytic activity of ZnO nanoparticles for the degradation of organic pollutants. *Materials Science and Engineering: C*, 33(1), pp.91–98.
 - Tauc, J., 1968. Optical properties and electronic structure of amorphous Ge and Si. *Materials Research Bulletin*, 3(1), pp.37–46.
 - Tseng, C.H., Baker, C.O., Shedd, B. and Kaner, R.B., 2007. Charge-transfer interactions in polyaniline/carbon nanotube composites. *The Journal of Physical Chemistry C*, 111(22), pp.7892–7897.
 - Wang, W., Tadé, M.O. and Shao, Z., 2015. Research progress of perovskite materials in photocatalysis and photovoltaics-related energy conversion and environmental treatment. *Chemical Society Reviews*, 44(15), pp.5371–5408.
 - Wang, Y., Jing, X. and Kong, J., 2010. Polyaniline-based nanocomposites: Preparation and application in photocatalysis. *Polymer International*, 59(6), pp.807–814.